Physical Characterization of Biobased Corrugated Panels, an Innovative Material

Adrien Gaudelas,[a,*] Pierre Blanchet,[a] Louis Gosselin,[b] and Matheus Roberto Cabral [a]

Corrugated panels possess excellent thermomechanical properties, but, with presently no hygrothermal applications for building envelopes, their full potential still needs to be explored. This study characterized the physical properties of three biobased corrugated compositions to identify potential building applications. Flat samples of the same compositions were analyzed for certain properties to aid in understanding. As this characterization is groundbreaking, the testing was based on or inspired by established standards. Results suggest that the panels with two wood veneer cores and two kraft paper surfaces coated with polymers are the most promising, as such structures are less sensitive to water and possess a good moisture buffer value that should be advantageous for building construction. Corrugated panels are particularly interesting because their inner materials have properties comparable to those of conventional wood-based panels such as plywood. However, the apparent properties of corrugated panels become one to ten times smaller or larger, which opens up new design possibilities for building envelope applications.

DOI: 10.15376/biores.18.3.5838-5858

Keywords: Biobased material; Corrugated panel; Hygrothermal properties; Wood-based panel.

Contact information: a: NSERC Industrial Research Chair on Eco-Responsible Wood Construction (CIRCERB), Department of Wood and Forest Sciences, Université Laval, 2425 Rue De La Terrasse, Quebec City, QC G1V 0A6, Canada; b: Department of Mechanical Engineering, Université Laval, Quebec City, QC G1V 0A6, Canada; Corresponding author: Adrien.gaudelas.1@ulaval.ca

INTRODUCTION

Corrugated composites are widely used in packaging due to their recyclability, low cost, strong mechanical properties, and energy-absorbing capabilities, which protect products (Garbowski *et al.* 2023; Mrówczyński *et al.* 2023). Research has been conducted to improve their hygrothermal properties by incorporating polystyrene in the cavities (Sasaki and Kato 1999; Gray-Stuart *et al*. 2019). Corrugated structures are also employed to promote heat exchange in systems bearing the same name (Iwai *et al*. 2006; Doo *et al*. 2012; Al Zahrani *et al*. 2020; Ajeel and Salim 2021). This kind of structure can be prepared from thin sheet materials that are initially flat; it is an advantageous low-cost process of mass production (Choi *et al.* 2012).

These materials are classified into three configurations: corrugated pipes, corrugated sheets, and corrugated panels. They are highly anisotropic, exhibiting high stiffness perpendicular to the corrugation direction but greater compliance along it, making them popular in industry and academic research. For example, Le and Goo (2019) developed different corrugated composites inspired by the peacock mantis shrimp (*Odontodactylus scyllarus*). Their study showed that the bio-inspired corrugated core sandwich structures achieved a 65% weight reduction without compromising deflection

limits. In addition, both materials exhibited similar thermal conductivity performance. Bapanapalli *et al*. (2006) suggested using corrugated sandwich panels as a thermal protection system for space vehicles against extreme aerodynamic heating due to their heat transfer and load-bearing capabilities.

Furthermore, corrugated materials are used to insulate hypersonic craft, such as rockets (Innocenti and Scarpa 2009; Ma *et al*. 2017; Shi *et al*. 2020; Chen *et al*. 2021). They are also used for marine applications such as structures, including the superstructure deck of a ship and radar platforms (Liu *et al*. 2022). Similar structures are used to design fire-resistant vehicles (Lurie *et al*. 2020). For construction purposes, metal-based corrugated structures are widely used as cladding for building envelopes (Cunha *et al*. 2015) and have also been studied as bracing in resisting seismic and wind loads (Zhang *et al*. 2016). However, the study of biobased corrugated structures for buildings is recent. For example, McCracken and Sadeghian (2018) and von der Heyden and Lange (2017) used corrugated cardboard to create beams as a core material in sandwich panels for building envelopes, and they specifically explored its mechanical properties as a core material in sandwich panels used for building envelopes. Furthermore, studies have been conducted on corrugated panels made from veneer scraps for structural applications (Denes *et al*. 2017a,b). Similarly, oriented strand board (OSB) sandwich materials with a corrugated core have also been investigated for their structural properties (Voth *et al*. 2015; Mohammadabadi *et al*. 2020).

Sattler and Österreicher (2019) developed an adaptive envelope retrofit system that uses corrugated cardboard to enhance solar heat gain in buildings during winter and decrease it during summer. In addition, Kittisak and Prayoon (2021) researched using corrugated panels made from sugarcane fiber as building cladding. Recently, Jiloul *et al*. (2023) investigated the mechanical resistance of wood-based corrugated panels made from wood veneers and fibers; their research has shown that this panel type can be used for building structural applications. However, although corrugated panels exhibit excellent thermo-mechanical properties that make them a promising building material for envelopes, their full potential has not yet been realized due to a lack of studies regarding their hygrothermal performance. Therefore, this study aims to characterize the physical properties of three compositions of biobased corrugated panels to identify potential building envelope applications.

EXPERIMENTAL

A set of tests were conducted to identify applications for bio-based corrugated panels as building envelope materials described in the following sections. To do so, two physical properties were investigated: firstly, those required for hygrothermal modeling (such as thermal conductivity, thermal capacity, water vapor permeance, water absorption coefficient, and sorption/desorption); and secondly, those that, when combined, enable the evaluation of the capabilities of the studied panels (such as moisture buffering capacity).

Materials

The corrugated panels studied were supplied by Corruven Inc. in Edmunston, NB, Canada. The study included three panels from two production series (A and B): CorrPack 1902, CorrShield 1904, and CorrShield 1910 Polyback. The selection of the panel depended on the specific test being conducted. The panel shown in Fig. 1a, identified by

the code "1902," comprises multiple layers of kraft paper. The panel (Fig. 1b) identified by the code "1904" is a sandwich panel comprising a wood veneer core of *Betula sp*. and two kraft paper surfaces. The panel (Fig. 1c) identified by the code "1910" is a sandwich panel comprising two wood veneer cores of *Betula sp*. and two kraft paper surfaces coated with polymers. In addition, tests were conducted on the flat versions for all panel series.

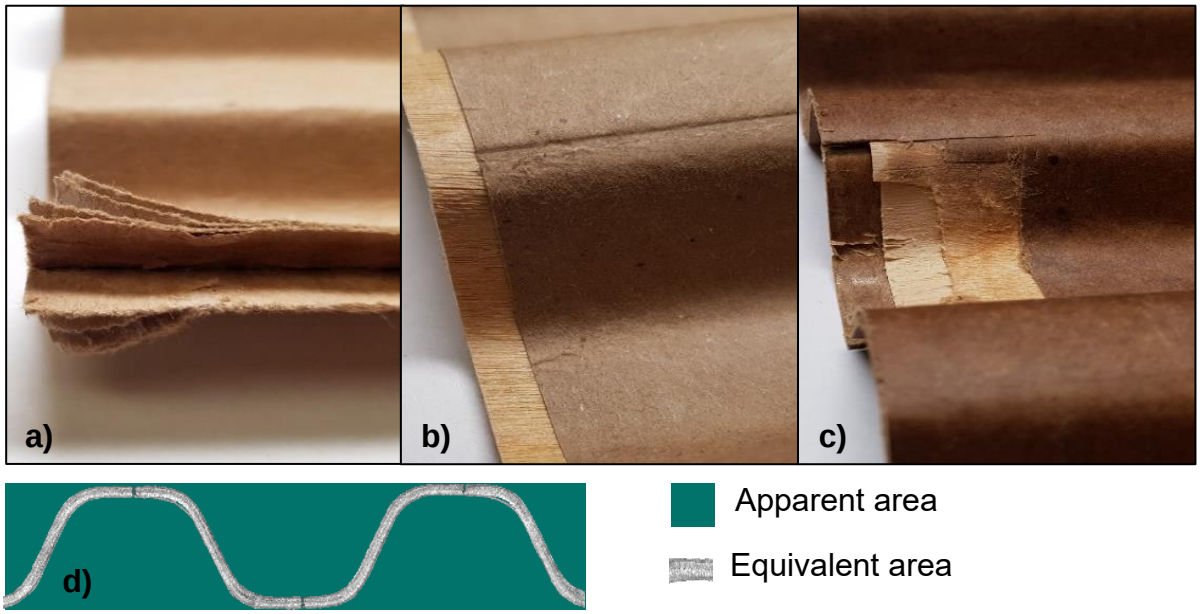

Fig. 1. Corrugated panels used in this study. a) Corrpack 1902; b) Corrshield 1904; c) Corrshield 1910 and d) Cross-sectional area considered in the study.

When characterizing corrugated panels, two types of properties depending on the selected section were considered, as shown in Fig. 1d. The first one is the cross-sectional area of the material alone, denoted as the equivalent area A_{eq} (m^2), which has a thickness of 1 to 2 mm (Table 1). The second is the cross-sectional area of the material and the space between the corrugations, named the apparent area A_{ap} (m^2), which has a flute height of 17.4 mm for 1902 and 19 mm for the 1904 and 1910, with a pitch of 55.5 mm for the 1902 panel and 50 mm for the 1904 and 1910 panels. The same measuring processes were used for the flat panels, with their properties denoted as x_f. The symbols x_{eq}, x_{ap}, and x_f were used to identify to which areas the physical properties refer to. Note that the manufacturing process described in this article is detailed in patent WO 2010/060219, Wave wood assembly and method of making same (Belanger and Blais 2010).

Table 1. Description of the Studied Corrugated Samples

Panel type	CorrShield 1902	CorrPack 1904	CorrPack 1910
Surface layer	Kraft paper	Kraft paper	Kraft paper polymer coated
Core layer	Kraft paper	One *Betula sp*. veneer	two *Betula sp*. veneers
Thickness	2 mm	1 mm	2 mm
Flute height	17.4 mm	19 mm	19 mm
Pitch	55.5 mm	50 mm	50 mm

Methods

Thermal conductivity of flat panels

To determine the thermal conductivity of the flat panels, the ASTM C 518 (ASTM International 2017) standard recommendations were followed with some modifications regarding the thickness of the material. Samples measuring 300 × 300 mm were used, and a TA Instrument heat flux meter FOX 314 version 89v (New Castle, DE, USA) was employed for the tests. The experiments were conducted using the fixed plate temperature method, and data were collected using Winth32v3 version 3.31.110 software. A reference sample of expanded polystyrene was used to calibrate the equipment before the test (ASTM International 2019a).

According to the standard recommendations, four temperatures T (°C) were set (*i.e.*, 12.5; 22.5; 32.5 and 42.5 °C). A temperature difference (ΔT) of 25 °C was chosen based on Table 3 of ASTM standard C 1058/C1058M (ASTM International 2015). For these determinations, 224 tests were conducted, with each flat panel type tested five times, three times in correction setups, for four mean temperatures and two moisture content levels. For the first series of tests, samples were stored in conditioning chambers at 20 °C and relative humidity (RH) of 40% RH ±1% RH until their mass changed by less than 1% in 24 h. The samples were conditioned the same way for the second series at 20 °C and 65% RH. Once the samples had been conditioned, the test was conducted at room temperature and humidity. Given the speed of the tests, it was assumed that the water content of the samples remained close to that obtained after conditioning.

Considering that the samples of the corrugated panels were very thin, the effect of the thickness on the thermal resistance obtained by the apparatus R_t (m.K.W^{-1}) was corrected (Tleoubaev and Brzezinski 2008). The correction used the two-thickness method by subtracting thermal resistance at the sample-apparatus interface to improve accuracy (Tleoubaev and Brzezinski 2008). The goal was to isolate the thermal resistance of the sample R_s and determine its thermal conductivity λ_s (W.m^{-1}.K^{-1}). Stacks with different numbers of panels were therefore tested, allowing determining in each case the total thermal resistance, including the resistance R_s, the resistance of the contact with the plates R_c, and the resistance of the interface between the samples R_i. To isolate λ_s, four stacks were considered, as shown in Fig. 2, with 1, d_{x1}, d_{x2}, and d_{x3} layers of samples, where d_{x1} was close to the calibration thickness of the apparatus (25 mm) and varied according to the material, d_{x2} had one more layer, and d_{x3} had two more layers. Neglecting R_i between panels, R_t, can be expressed by Eq. 1.

$$R_t = nR_s + R_c = \frac{d}{\lambda_s} + R_c \quad (1)$$

R_t was plotted as a function of the stack thickness. Then, the slope of the regression is equal to $1/\lambda_s$.

Before applying the method to corrugated panels, which had no existing results in the literature, it was evaluated using dummies, specifically High-Density Fiberboard (HDF). The direct results of the thermal conductivity of HDF obtained from the heat flow meter were about 0.0816 ± 0.0022 W.m^{-1}.K^{-1}, but this value contains a systematic error. For the same material, with a density of about 1000 kg.m^{-3} and a moisture content (MC) of about 6 to 7% MC, Kawasaki *et al*. (1998) determined a thermal conductivity of about 0.17 W.m^{-1}.K^{-1} using a heat flow meter. Applying the correction method shown in Fig. 2 to the HDF results yielded a thermal conductivity value of 0.1629 W.m^{-1}.K^{-1}, which was closer to the value reported by Kawasaki *et al*. (1998), with a difference of only 4% that could be

due to reproducibility variation, or the interface resistance R_i. This value was also by the results of Zahedsheijani *et al*. (2012) on a less dense fiberboard (750 kg.m^{-3}) that was conditioned at a higher RH and had a thermal conductivity of 0.149 W.m^{-1}.K^{-1}.

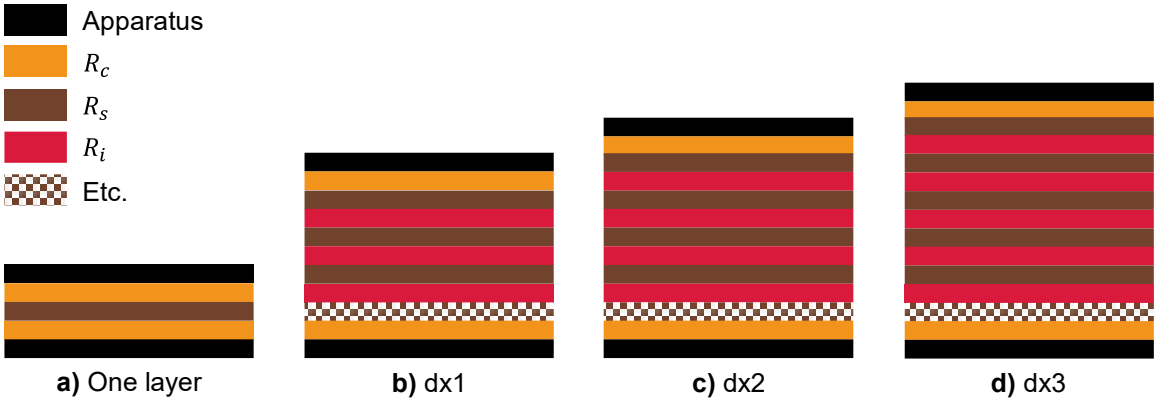

Fig. 2 Test setup scheme for thermal conductivity correction

Heat capacity of panels

The heat capacity of the flat panels was determined following the recommendations of the ASTM standard E 1269 (ASTM International 2018), with the help of a Mettler Toledo 822/e differential scanning calorimeter (DSC) from Columbus, OH, USA. This method uses a reference synthetic sapphire sample selected for its minor deviation and good reproducibility (Nopens *et al*. 2021). The DSC analysis comprised three programmed segments. Firstly, an initial isotherm of 3 min at -30 °C, followed by a second dynamic segment with a substandard heating rate of 10 °C/min. Lastly, a final 3-minute isothermal step at 40 °C was conducted.

To conduct the tests, 10 samples were used, one from sapphire and nine from corrugated panels cut into 5 mm diameter disks for each panel and placed into crucibles with a volume of 40 µL. Before the tests, the samples were stored in a conditioning chamber at 20°C and 65% RH ±1% RH until their mass changed by less than 1% in 24 h. The tests involved heating the material and measuring its internal energy D (W) as a function of temperature T from [-30°C ; 40°C]. The blank measurement was first performed, then subtracted from the sample measurement to eliminate the crucible's effect.

The internal energy values of the samples were then normalized concerning their masses D_n (W.g^{-1}). The heat capacity Cp_f (J.g^{-1}.K^{-1}) was subsequently calculated using the following formula Eq. 2,

$$Cp_f = Cp_{st,s} \frac{D_{n,f}}{D_{n,s}} \quad (2)$$

where the standard heat capacity of synthetic sapphire, denoted as $Cp_{st,s}$ (J.g^{-1}.K^{-1}), was obtained from Table 1 of ASTM standard E 1269 (ASTM International 2018). The specific internal energy of the panel samples and the specific internal energy of the synthetic sapphire sample was represented by $D_{n,f}$ (J.g^{-1}) and $D_{n,s}$ (J.g^{-1}), respectively.

Water absorption coefficient by partial immersion of flat and corrugated panels

The water absorption coefficient of the panels was determined using a partial immersion method with a modified version of ASTM standard C 1794 (ASTM International 2019b). The material tested is anisotropic, so testing was conducted on two

orientations corresponding to corrugations aligned vertically and horizontally. In addition, two orientations of the flat panels (1904$_f$ and 1910$_f$) were tested corresponding to fiber orientations in the veneers of the panels aligned vertically and horizontally. To ensure that the test was representative, the apparent surface area of the panels' samples A_{ap} was set to about 60 cm². The experiment was carried out on 36 corrugated samples, comprising three repetitions in two directions for two production series of three types of panels measuring 400 × 300 mm. Additionally, 25 flat samples were tested, with five repetitions in two directions (except for 1902, which does not have a fibers orientation) for three types of panels measuring 400 × 300 mm.

Before the tests, the samples were conditioned at 20°C and 65% RH ± 1% RH in a conditioning chamber until their mass changed by less than 1% in 24 h. Subsequently, the samples were maintained under the same conditions throughout the tests. The vertical sides of the samples were sealed using a plastic film due to the non-flat nature of the samples. In addition, the horizontally corrugated samples were vertically wrapped with five nylon fishing lines to avoid deformation. The experiment lasted 24 h, and the sealant's effectiveness was checked to verify its performance.

The standard procedure involves weighing each sample before immersion to determine its initial mass m_i (kg). Additional weight measurements should be taken at 5, 30 min, 1, 2, 4, 8, and 24 h, with water removed from the sample before each weighing. However, this method may have flaws, as Zelinka *et al.* (2016) and Lu *et al.* (2020) noted. The first concern is that removing the sample from the water may disrupt the capillary mechanism in the sample, while the second is that handling the sample in water may cause water to contact an area of the sample outside the allowable tolerances. To address these issues, as shown in Fig. 3 a) and b), the samples were suspended from a scale with a resolution of ± 1 mg and immersed for 24 h. The Wedge v1.2 data acquisition system recorded the mass evolution every 5 min.

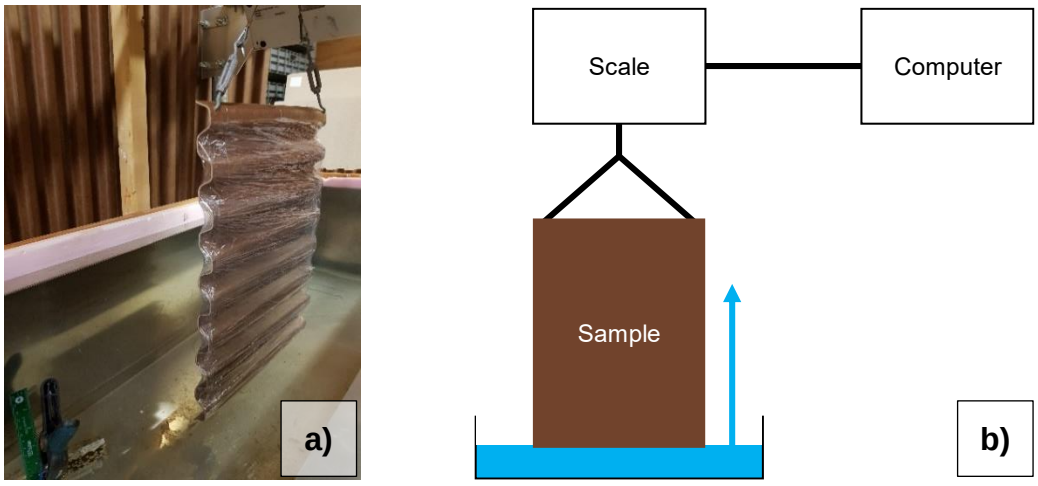

Fig. 3 a) test setup of water absorption coefficient by partial immersion test; b) test setup scheme

The measured mass of each sample was first normalized by its apparent cross-section area A_{ap}, or A_f for flat samples. Then, the normalized mass was plotted against the square root of time $\sqrt{t}$ ($s^{-0.5}$). The water absorption coefficient A_w is simply the slope of the linear segment of that curve. In this work, the slope between t = 2 h and t = 24 h was

generally used, as data points before 2 h correspond to an initial regime, not aligning with the expected linear profile.

Water vapor permeance of corrugated and flats panels

The water vapor permeance of the panels was determined in the spirit of the ASTM standard E 96/96M, Procedure B-Water method at 23°C (ASTM International 2016a). Plexiglas sheets were cut and joined to form boxes with an interior base surface area of 200 x 200 mm. The joints of the boxes were then sealed using liquid paraffin. A total of 39 samples were tested, which included three repetitions of two production series of three types of corrugated panels, three repetitions of three types of flat panels, three repetitions of control samples fully coated with sealants, six control samples of WallShield IT Integrated Tape Product No.: 40105500 / 40108000 from VaproShield (whose results were compared with those provided by the manufacturer), and three repetitions with 0.640 mm thick aluminum plate. The surface area tested per sample was 0.0196 m².

The samples were cut to dimensions of 200 × 200 mm. As the tested panels were not flat, the standard sealing method was modified accordingly. The edges of the samples were dipped into a bath of liquid paraffin (30 ± 1 mm in depth) near its melting point (between 50 and 57 °C) to prevent migration (Fig. 4 a); b) and c)). Sealing the area with paraffin made a more precise and accurate measurement of the water vapor permeable surface between the samples possible. The surface area *A* and thicknesses *d* of the samples were determined by scanning them using an EPSON EXPRESSION 1640XL MODEL G650C scanner at a resolution of 1000 pixels per inch. The images were then analyzed using ImageJ v1.53k. To ensure uniformity in the testing environment, all the samples were conditioned at 23°C and 50% RH ± 1% RH until their mass changed by less than 1% in 24 h. The tests were conducted in an environment with the same conditions.

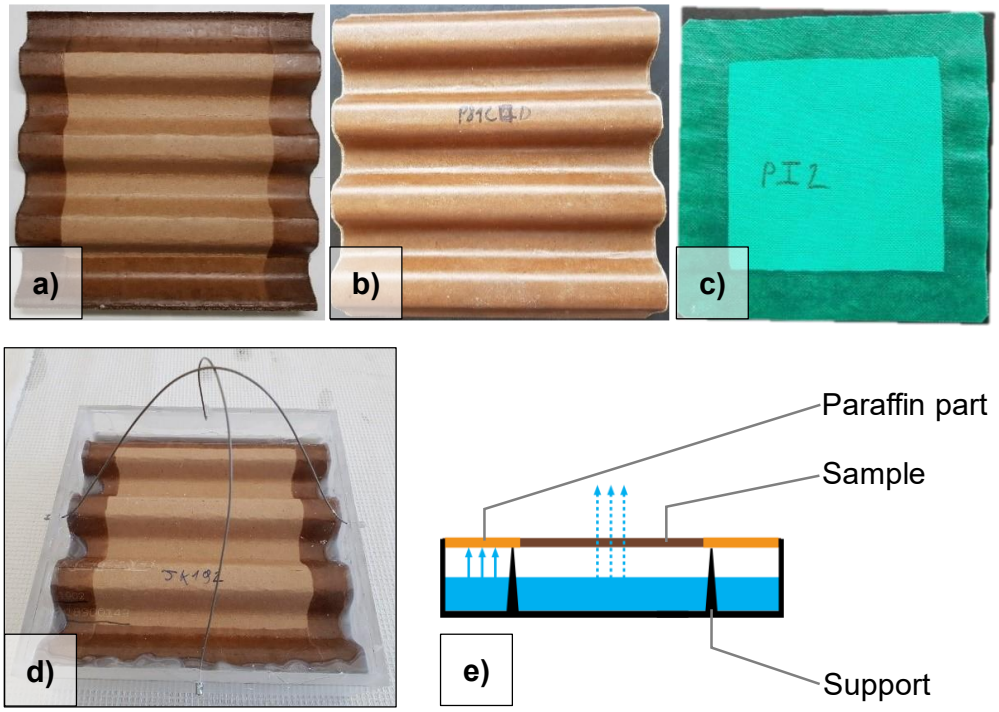

Fig. 4. a) 1902 sample with sealed edges; b) fully sealed 1910 control sample; c) weather barrier control sample; d) Permeance test setup; e) cross-sectional scheme of the test setup

To initiate the test, the boxes were filled with distilled water until they reached a distance of 19 ± 6 mm from the sample. Subsequently, the samples were placed in the box and sealed with Superbonder 735 hot melt, as shown in Fig. 4 d) and e).

Then, the samples were weighed with a laboratory scale with a resolution of ± 1 mg at the beginning of the test and every 24 h. During the weighing process, a graph was plotted to depict the evolution of the mass G (g) of the samples in grams as a function of time t (h). Finally, the test ended when six consecutive weightings aligned on the linear regression line of the points on the graph, indicating that the flow of water vapor had reached a steady state.

The water vapor transmission WVT ($g.h^{-1}.m^{-2}$) was calculated using Eq. 3.

$$WVT = \frac{G}{t.A} \quad (3)$$

The apparent water vapor permeance (perm) was calculated using Eq. 4,

$$Permeance = \frac{WVT}{\Delta P} = \frac{WVT}{P_{sat}(\varphi_1 - \varphi_2)} \quad (4)$$

where P_{sat} (Pa) represents the water vapor pressure at saturation, φ_1 (% RH), the relative humidity in the box, and φ_2 (% RH), the ambient relative humidity.

The water vapor permeability δ ($g.s^{-1}.m^{-1}.Pa^{-1}$) was calculated using Eq. 5,

$$\delta = Permeance \times d \quad (5)$$

where d (m) is the thickness of the samples.

Both tests of the flat and corrugated samples showed that the fully paraffined corrugated panels and the aluminum plate had results close to or equal to 0 perm, indicating that the sealing system designed for the test can be considered effective and impermeable to water vapor. Moreover, the coefficient of variation of reproducibility of the ASTM standard is between 13.4% and 21.8% (ASTM International 2016a). The results obtained for the weather membrane with 118.5 ± 4.1 and 126.4 ± 2.0 perm for two series of tests carried out (one of the corrugated samples and one of the flat samples) also confirm the robustness of the method, as the value is consistent with that given by the company VaproShield of 123 perms (VaproShield LLC 2022).

Dynamic vapor sorption of panels

The Dynamic Vapor Sorption **(**DVS**)** of panels was determined using the ASTM standard C 1498 – 04a as a basis (ASTM International 2016b), along with the DVS application notes N° 61 (Acharya *et al*. 2014) and N° 104 (Burnett *et al*. 1996). The measurement was conducted using a dynamic vapor sorption equipment, the DVS Adventure from SMS, London, UK.

The samples were cut into disks of 5 mm diameter. Three replicates were taken for each of the three types of panels, resulting in a total of nine samples. In preparation for the test, the samples were oven-dried at 103 °C for 24 h to ensure they were anhydrous. In addition, the apparatus was calibrated with a salt validation, a pressure check, and a scale calibration. An isothermal dynamic sorption method was developed for 25 °C on the apparatus. After an initial drying step for 2 h at 0% RH, the samples were exposed to a series of steps ranging from 0 to 95% RH and then to the same series in reverse order. The steps were 10% RH increments, except between 90% RH and 95% RH. The device progressed to the next step, when the mass of the sample varied by less than 0.002% for 10

min. The equipment measured the mass of the samples with a resolution of ± 3 µg up to the hundredth minute.

The test involved recording the change in mass of the samples for the relative humidity to determine the humidity content *u* (% MC) of the samples using Eq. 6,

$$u = \frac{m_n - m_a}{m_a} . 100 \quad (6)$$

where m_n (mg) is the mass of the sample at equilibrium for the RH level *n* and m_a (mg), is the anhydrous mass of the samples. The value of m_a, was measured after the 2 h step at 0% RH.

Moisture buffer value of corrugated panels

The moisture buffering capacity of corrugated panels was determined following the recommendation of NORDTEST standard Water buffering capacity project (Rode *et al*. 2005). It was inspired by the ISO standard 24353: 2008(E) (International Organization for Standardization 2008).

Nine samples measuring 100 mm x 100 mm were prepared, consisting of three replicates for each panel type. Before the tests, the samples were stored in a conditioning chamber at 20 °C and 65% RH ±1% RH until their mass changed by less than 1% in 24 h. The samples were sealed on five of their six sides, leaving only one unsealed side for moisture exchange with the environment. The chamber was programmed to perform four isothermal cycles at 23°C for 24 h. These cycles consisted of 8 h of sorption at 75% RH, followed by 16 h of desorption at 50% RH. The samples were placed on the scale, unsealed side up, and the cycles were initiated. Mass readings were taken every 5 min during the four cycles using Winth32v3 version 3.31.110 software.

Average of the last four mass readings was used to calculate the moisture buffer value MBV_{ap} (g.m^{-2}.% RH^{-1}), as shown in Eq. 7,

$$MBV_{ap} = \frac{m_{4s} - m_{3d}}{A_{ap}.\Delta\%\,RH} \quad (7)$$

where m_{4s} (g) represents the average mass of the samples at the end of the fourth sorption cycle at 75% RH, m_{3d} (g), the average mass of the samples at the end of the third desorption cycle at 50% RH, and Δ% RH the difference in relative humidity between the sorption and desorption cycle.

RESULTS AND DISCUSSION

Thermal Conductivity of Flat Panels

The thermal conductivity of samples exhibited a linear relationship that depended on the test temperature and moisture (Fig. 5) typical of wood-based materials.

Thermal conductivity results are presented below at a mean temperature of 22.5 °C, where the %RH corresponds to the %RH of conditioned samples in Fig. 5. The lowest value was observed for 1902 panels at 0.0787 W.m^{-1}.K^{-1} and 0.0874 W.m^{-1}.K^{-1} for conditioning at 20°C and 40% RH and 65% RH, respectively. It should be noted that the two relative humidity points seem to converge for higher temperatures. The 1904 panel showed results similar to those obtained from the 1902 panel, with a thermal conductivity of 0.0923 W.m^{-1}.K^{-1} at 40% RH and 0.0902 W.m^{-1}.K^{-1} at 65% RH. In contrast, the 1910 panels exhibited the highest thermal conductivity values at 0.1118 W.m^{-1}.K^{-1} at 40% RH

and 0.1326 $W.m^{-1}.K^{-1}$ at 65% RH. These observations suggest that thermal conductivity is positively influenced by the proportion of wood veneer and negatively influenced by the proportion of cardboard. Furthermore, despite the variations in their thermal conductivity values, the panels showed potential as insulation materials for applications that prioritize thermal comfort, since their values were below the threshold of 0.25 W/mK, as indicated by Zhou *et al*.'s definition of thermal insulation materials (Zhou *et al*. 2010).

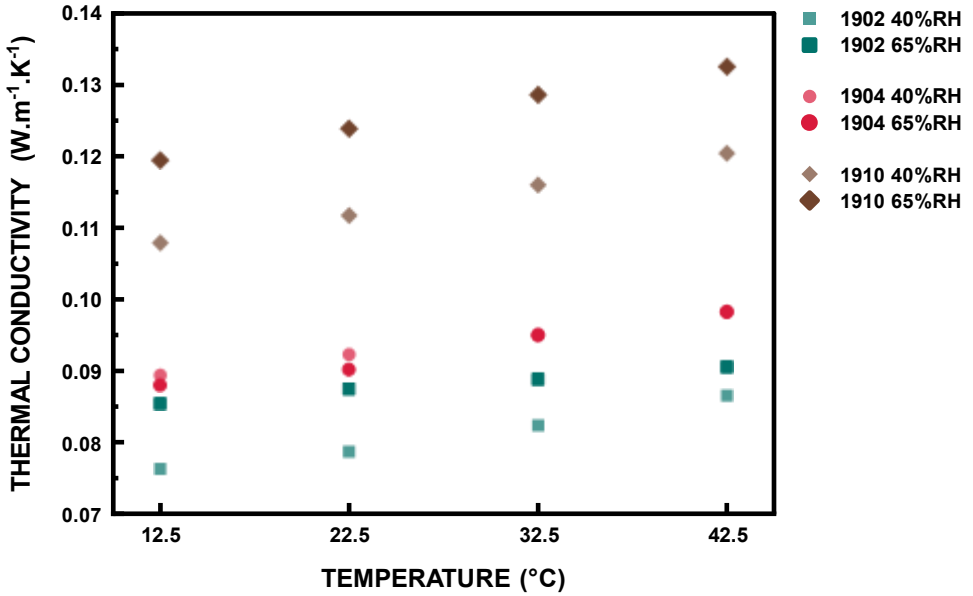

Fig. 5. Corrected thermal conductivity of flat panels

Heat capacity of panels

The measured heat capacity of the panels is shown in Fig. 6. The results indicate that the heat capacity of the samples increased with rising temperatures, in agreement with previous studies on wood-based materials (Dupleix *et al*. 2013; Mvondo *et al*. 2020; Radmanović *et al*. 2014; Rice and Redfern 2016). Variations in the heat capacity of materials could be attributed to side effects caused by moisture gradients, water diffusion or evaporation, and the moisture content of the wood-based materials (Dupleix *et al*. 2013; Mvondo *et al*. 2020; Radmanović *et al*. 2014).

The values presented below correspond to the average obtained at 23.83°C. In Fig. 6, the heat capacity of 1902 panels at 9.92% MC was found to be higher at $(1.98 \pm 0.05)\times10^3$ $J.kg^{-1}.°C^{-1}$ than 1904 panels at $(1.88 \pm 0.03)\times10^3$ $J.kg^{-1}.°C^{-1}$ for 15.98% MC, which in turn had a higher heat capacity than 1910 panels at $(1.65 \pm 0.10)\times10^3$ $J.kg^{-1}.°C^{-1}$ for 9.81% MC. It should be noted that, between 30 and 40°C, the heat capacity of the 1902 and 1904 panels was similar. The heat capacity also increased with the proportion of kraft paper and decreased with the wood veneer in the samples. This could be due to various amounts of wood compounds, such as lignin, cellulose, and hemicelluloses, which have different thermal capacities, as Sonderegger *et al.* (2011) reported.

The heat capacity of the 1910 panels was comparable to those reported for plywood panels by Rice and Redfern (2016), which was a value of 1.42×10^3 $J.kg^{-1}.°C^{-1}$ for 9.41% MC. However, the difference with the present results can be attributed to the different methods used by Rice and Redfern (2016) (*i.e*., drop calorimetry), the differences in the composition of the materials tested, and the lower temperature used in their study.

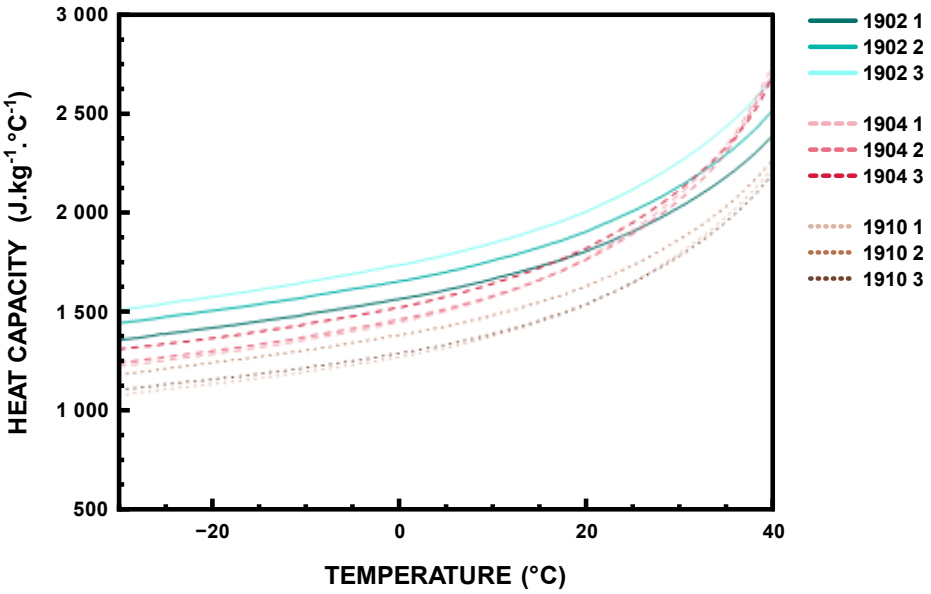

Fig. 6. Heat capacity of panels and sapphire dummy as a function of the temperature

The results obtained for the 1902 panels were significantly higher than those Adl-Zarrabi and Boström (2004) reported for a less dense material under lower temperature and moisture content conditions. Similarly, Klinklow *et al*. (2013) found lower results for these same types of panels. Although Klinklow *et al*. (2013) used the same method (DSC), they did not apply the sapphire correction or specify the temperature and humidity conditions used in their experiments. In contrast, the results for the panels were more comparable to those reported by Czajkowski *et al*. (2016) for fiberboard, where the temperature and moisture content of the samples were lower. Therefore, although some differences in the results could be observed when compared to the literature, they fell within similar data ranges, and the variations can be attributed to differences in material composition, parameters, and test methods.

Water absorption coefficient by partial immersion of flat and corrugated panels

Generally, these behaviors include a first phase in the transient state, which lasts approximately 80 $s^{-0.5.}$ After this period, the transfer becomes steady or quasi-steady. This transient phase can be attributed to other liquid water transfer phenomena, such as diffusion. Therefore, most water absorption coefficients are calculated over the interval 80 to 294 $s^{-0.5}$ or 2-24 h, as seen in the methodology section, and are presented in Table 2.

The panels 1910_{ap} panels were found to be the least sensitive to the capillary mechanism, with a water absorption coefficient of 0.0050 ± 0.0004 $kg.m^{-2}.s^{-0.5}$ in vertical orientation and 0.0013 ± 0.0004 $kg.m^{-2}.s^{-1/2}$ in horizontal orientation, absorbing about ten times less water than the 1902_{ap} and 1904_{ap} panels. Water can thus rise through the surfaces of the 1904_{ap} panel by capillarity, explaining why these results are similar to the 1902_{ap} panels. In this case, the wood veneer cores have little influence on the results. This is confirmed by the results of the 1910_{ap} panel, which is covered by a polymer that does not allow the capillary mechanism to occur, resulting in a low general result. It also confirms that the wood veneers do not positively influence the capillary mechanism in those panels. Comparing the equivalent and flat area results, the horizontal corrugation process increases

the material's propensity to absorb water. This confirms that the orientation of the material relative to gravity affects the water absorption of the panel. Among the flat panels (Table 2. Water absorption coefficients of corrugated samples), the 1910_f absorbed the least amount of water, with a water absorption coefficient of 0.0398 ± 0.0043 kg.m^{-2}.s$^{-1/}$2 and 0.0159 ± 0.0021 kg.m^{-2}.s$^{-1/2}$ in vertical and horizontal orientations, respectively. For the flat version, the results of the 1902_f and 1904_f panels was not confounded, with the 1902_f panel being the most absorbent.

Table 2. Mean Value and Standard Deviation of Water Absorption Coefficients of Corrugated Samples

Panel	Area	Orientation	Water Absorption Coefficient (kg.m^{-2}.s$^{-0.5}$)		
			Batch A	Batch B	General
1902	Ap	Vertical	0.0596 ± 0.0019	0.0241 ± 0.0016	0.0419 ± 0.0195
		Horizontal	0.0636 ± 0.0026	0.0155 ± 0.0009	0.0395 ± 0.0264
	Eq	Vertical	0.5423 ± 0.0112	0.2311 ± 0.0167	0.3867 ± 0.1709
		Horizontal	0.7168 ± 0.0327	0.1920 ± 0.0156	0.4544 ± 0.2884
	f	Isotropic			0.5960 ± 0.0385
1904	Ap	Vertical	0.0321 ± 0.0055	0.0340 ± 0.0013	0.0330 ± 0.0037
		Horizontal	0.0261 ± 0.0018	0.0265 ± 0.0022	0.0263 ± 0.0018
	Eq	Vertical	0.2948 ± 0.0205	0.4196 ± 0.0172	0.3572 ± 0.0704
		Horizontal	0.4618 ± 0.0364	0.4823 ± 0.0421	0.4721 ± 0.0369
	f	Vertical			0.4272 ± 0.0453
		Horizontal			0.1102 ± 0.0147
1910	Ap	Vertical			0.0050 ± 0.0004
		Horizontal			0.0013 ± 0.0004
	Eq	Vertical			0.0381 ± 0.0018
		Horizontal			0.0134 ± 0.0035
	f	Vertical			0.0398 ± 0.0043
		Horizontal			0.0159 ± 0.0021

The results of the equivalent area of the corrugated samples and the flat panels are not compared, as those results have no tendencies. Compared to the results of Sonderegger *et al*. (2012) for plywood, the results of the 1910_{eq} and 1910_f panels were superior for the vertical orientation and inferior for the horizontal orientation. This is attributable to the wood's anisotropy, since the plywood veneers are crossed, unlike in the corrugated panels. Comparing the results of Sonderegger *et al*. (2012) for fiberboards, the 1902_f panels were also ten times inferior. Therefore, comparing the results of the 1902_f panels and fiberboards is difficult for water absorption.

Water vapor permeance of corrugated and flat panels

The results for water vapor permeability results of flat and corrugated samples are presented in Table 5. For the flat panels, the results showed that 1910_f panels were the least permeant with 14.20 ± 1.23 perm. On the other hand, the permeability of the panels 1904_f at 1.497 ± 0.099 ng.s^{-1}.m^{-1}.Pa^{-1} and 1910_f at 1.540 ± 0.182 ng.s^{-1}.m^{-1}.Pa^{-1} were confounded. This means that since the polymer coating has a small thickness for the flat samples, it has an insignificant influence on the water vapor transfers. Adding a veneer from the 1902f to the 1904f panel and then a second one from the 1904f to the 1910f panel will decrease the permeability.

Table 3. Mean Value and Standards Deviation of Water Vapor Transmission Rate, Water Vapor Permeability, and Permeance Results of Flat and Corrugated Samples

Sample	Thickness	WVT	Permeability	Permeance
	mm	$g.m^{-2}.h^{-1}$	$ng.s^{-1}.m^{-1}.Pa^{-1}$	perm
1902_f	1.542 ± 0.016	13.08 ± 1.26	3.991 ± 0.387	45.28 ± 4.37
1904_f	1.080 ± 0.019	7.002 ± 0.394	1.497 ± 0.099	24.24 ± 1.36
1910_f	1.894 ± 0.058	4.102 ± 0.355	1.540 ± 0.182	14.20 ± 1.23
$1902_{A,ap}$	18.591 ± 0.316	15.48 ± 0.91	56.96 ± 4.19	53.59 ± 3.16
$1902_{B,ap}$	18.797 ± 0.154	15.91 ± 0.30	59.16 ± 1.49	55.08 ± 1.03
1902_{ap}	18.694 ± 0.249	15.69 ± 0.65	58.06 ± 3.06	54.34 ± 2.25
$1904_{A,ap}$	19.005 ± 0.999	12.24 ± 0.44	45.96 ± 0.75	42.38 ± 1.51
$1904_{B,ap}$	18.046 ± 0.189	15.01 ± 0.33	53.61 ± 1.73	51.98 ± 1.14
1904_{ap}	18.525 ± 0.830	13.63 ± 1.56	49.79 ± 4.36	47.18 ± 5.40
$1910_{A,ap}$	19.847 ± 0.375	6.990 ± 0.294	27.45 ± 1.15	24.20 ± 1.02
$1910_{B,ap}$	20.409 ± 0.652	7.029 ± 0.074	28.39 ± 1.20	24.34 ± 0.26
1910_{ap}	20.128 ± 0.567	7.009 ± 0.193	27.92 ± 1.17	24.27 ± 0.67
$1902_{A,eq}$	1.493 ± 0.045	12.16 ± 0.72	3.589 ± 0.146	42.11 ± 2.49
$1902_{B,eq}$	1.418 ± 0.037	12.50 ± 0.23	3.507 ± 0.151	43.28 ± 0.81
1902_{eq}	1.455 ± 0.055	12.33 ± 0.51	3.548 ± 0.140	42.69 ± 1.77
$1904_{A,eq}$	0.966 ± 0.072	8.741 ± 0.311	1.669 ± 0.091	30.27 ± 1.08
$1904_{B,eq}$	0.948 ± 0.021	10.72 ± 0.24	2.011 ± 0.071	37.13 ± 0.82
1904_{eq}	0.957 ± 0.048	9.73 ± 1.11	1.840 ± 0.201	33.70 ± 3.85
$1910_{A,eq}$	1.848 ± 0.042	4.993 ± 0.210	1.824 ± 0.035	17.29 ± 0.73

For the corrugated panels, the apparent water vapor permeance measurements are reported in Table 5. Results indicate that the 1910_{ap} panels, considering A and B production batches, had an apparent permeance of 24.27 ± 0.67 perms, which was lower than the permeance of the 1902_{ap} panels at 55.08 ± 1.03 perm and 1904_{ap} panels at 47.18 ± 5.40 perm. The two production runs of 1904_{ap} panels also showed a significant difference, with 42.38 ± 1.51 perms for the A series and 51.98 ± 1.14 perms for the B series. In contrast to the flat sample test, the 1910_{ap} samples indicate that permeability and permeance were lower than those of the 1904_{ap} panels. The results for the 1904_{ap} panels were closer to those of the 1902_{ap} panels.

Vololonirina and Perrin (2016) suggest that the air layer water vapor resistance between the water and the sample did not have a significant effect on the results and that the shape of the samples did not significantly impact the tests. However, the reproducibility variation between 1904_{eq} and 1904_f, at 28.07%, and 1910_{eq} and 1910_f, at 22.11%, was much higher for their equivalent permeance than their flat version. These results suggest that, through the corrugation process, panels containing a core layer of wood veneers lost some of their water vapor resistance through corrugation process.

Compared to the results of Copak *et al*. (2022) on plywood, the results of the corrugated flat versions, 1910_f, were close. However, the apparent water vapor permeability results were more than ten times higher (Copak *et al*. 2022). No data are available to compare the results of panel 1902 in the literature. The corrugated panels were inherently more permeable to water vapor and ten times more permeable than other wood-based panels when in a corrugated shape.

The dynamic vapor sorption of panels

The results of the samples' dynamic sorption/desorption isotherm test are presented in Fig. 7. The results found for the studied panels showed a typical type 2 sigmoid shape characteristic of wood products (Skaar 1988). Panel 1902 showed a higher affinity for water vapor at 50% RH and 90% RH, with 5.91% ± 0.04% MC and 13.55% ± 0.14% MC, respectively, compared to other panel types. This behavior can be attributed to the easy formation of initial single-layer water-absorbed molecules below 20% RH (Skaar 1988; Pinterić 2017).

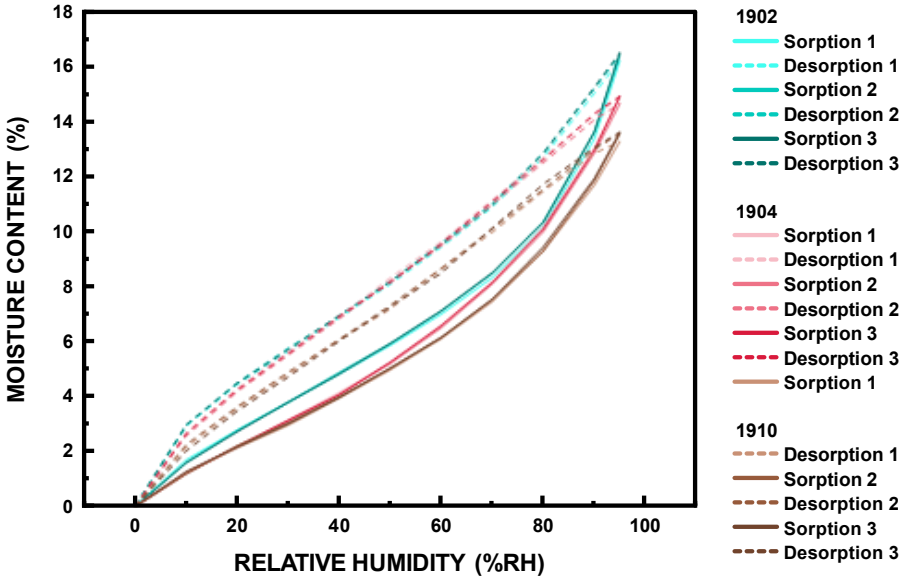

Fig. 7. Dynamic sorption/desorption isotherm of panels

Almeida *et al*. (2018) state that cellulose and hemicellulose are more hydrophilic than lignin because they contain more hydroxyl groups. Kraft paper mainly comprises cellulose and hemicellulose, so the varying amounts of kraft paper in panels 1902, 1904, and 1910 partially explain their different sorption results. However, this difference was not constant between 1902 and 1904 panels, with 5.23% ± 0.02% MC and 12.96% ± 0.09% MC, respectively. Between 45% RH and 75% RH, the moisture content of panels 1904 increased faster and joined the moisture content of panels 1902. This increase for panel 1904 can be attributed to the facility for water molecules to form multiple layers inside it, as Pinterić (2017) and Skaar (1988) described again. For Almeida *et al*. (2018), the sorption behavior at higher RH values is due to the size of its micropores, which should explain the end behavior of panels 1902 and 1904. Still, panel 1910 was the least hydrophilic, with 5.02% ± 0.03% MC and 11.83% ± 0.12% MC. There is not much literature on the dynamic sorption of plywood or fiberboard, so comparing the present results is challenging. The results for 50% RH correspond to Kumaran *et al*.'s (2006; 2010) findings on plywood, but for 90% RH, they were about 4 to 7% MC lower. The same observations are made when comparing 1902 panels to Kumaran *et al*.'s (2006; 2010) results on fiberboards. The difference in methods or material composition could explain this difference in moisture content at higher humidity. Generally, the dynamic vapor sorption results of the panels tested align with previous studies.

Moisture buffer value of corrugated panels

Figure 8 a) shows each panel type's normalized mass by surface area for the third desorption and the fourth sorption cycles. The curves of the 1902 and 1904 panels tended towards an asymptote at the end of each phase. The 1902 and 1904 panels were close to their moisture equilibrium during the dynamic sorption process. In contrast, the curve of the 1910 panels was constantly in progress, indicating that the 1910 panels were far from the equilibrium. As Ge *et al*. (2014) stated, the polymer in 1910 seemed to be the principal cause of this behavior. In Fig. 8 b), The moisture buffer capacity of panel 1910 was 1.12 ± 0.05 $g.m^{-2}.h^{-1}.\%\ RH^{-1}$, higher than the panel 1902 at 0.94 ± 0.05 $g.m^{-2}.h^{-1}.\%\ RH^{-1}$ and panel 1904 at 0.85 ± 0.04 $g.m^{-2}.h^{-1}.\%\ RH^{-1}$.

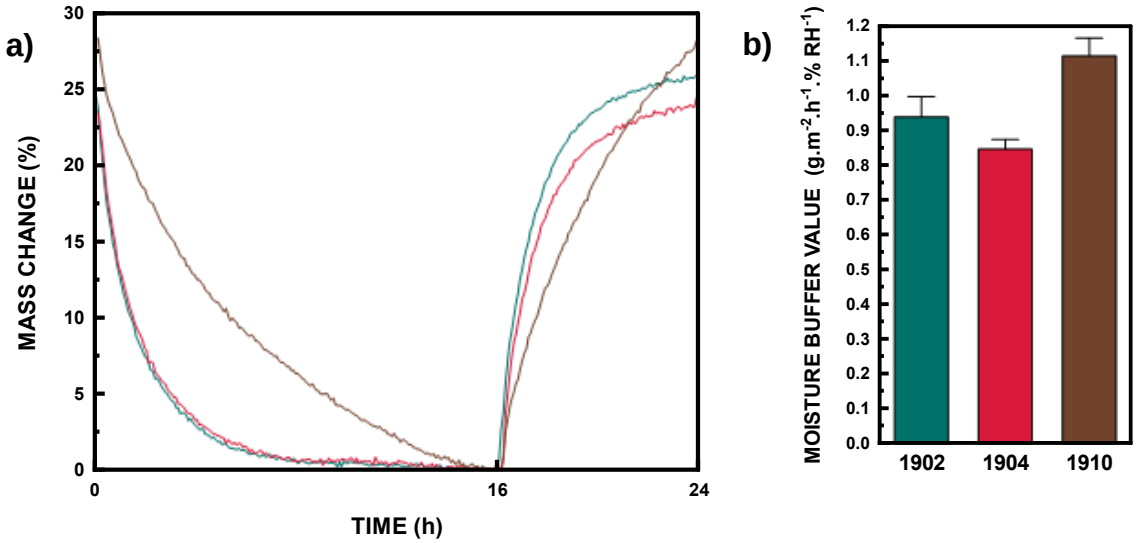

Fig. 8. a) Normalized mass of corrugated panels in the third desorption cycle and fourth sorption cycle; b) Moisture buffer value of corrugated panels

Ge *et al*. (2014) and Carmeliet *et al*. (2005) showed that water penetration depth influences the material's moisture buffer value. Thus, its lower equivalent thickness can explain the lower MBV value of 1904 panels. Compared to the results of Zhang *et al*. (2017) on wood fiberboard, the corrugated panels showed lower moisture buffer values. The results of Wu *et al*. (2008) confirmed this assumption with their results on fiberboard, which were even higher. However, the moisture buffer value of plywood reported by Wu *et al*. (2008) is about one-third of corrugated panels or about two-thirds of the results of Osanyintola *et al*. (2006).

It is important to note that although the apparent thickness of the corrugated panels was about 20 mm, their equivalent thickness was between 1 and 2 mm. Despite containing a much smaller quantity of material than those tested by Wu *et al*. (2008) and Osanyintola *et al*. (2006), the corrugated panels still had a high moisture buffer value. This is due to the shape of the corrugated panels, which increases the contact surface with the ambient air, so the mass of the material is close to its surface. Thus, biobased corrugated materials are an effective way to obtain high moisture buffer values.

With properties similar to plywood, these materials could be adapted for similar applications in the construction industry. Furthermore, their unique corrugated shape results in altered properties, presenting new design possibilities and potential applications.

CONCLUSIONS

1. The developed correction method for measuring the thermal conductivity of thin materials with a heat flow meter gave satisfactory results. Corrugated panels in their flat version exhibited a thermal conductivity within the range of fiberboards at 0.105 $W.m^{-1}.K^{-1}$ and plywood at 0.173 $W.m^{-1}.K^{-1}$ (Sonderegger and Niemz 2009), as they are composed of both veneers and fibers.
2. The heat capacity measurement confirmed that bound water in wood-based materials did not exhibit changing phase enthalpy, and this behavior was consistent even for processed fibers, such as kraft paper. Corrugated panels exhibited typical wood-based behavior for heat capacity in their inner material. Although the literature is inconsistent, the heat capacity identified for corrugated boards was close to the literature, with 1910_f panels being at least 17% higher than plywood under different conditions (Rice and Redfern 2016).
3. For the water absorption test, more precise weighing enabled better determination of whether the test was in a steady state or quasi-steady state transfer during analysis. The water absorption test also showed that this layer strongly influenced multilayer materials containing one layer with a higher water absorption coefficient. Corrugated panels in their flat version exhibited water absorption coefficients comparable to plywood ones when their fibers were oriented parallel to water uptake. 1910_f panels showed a 28% higher water absorption coefficient in this situation than plywood (Sonderegger and Niemz 2009).
4. Corrugated panels in their flat version had water vapor permeability close to that of plywood, as seen for 1910f (Copak *et al*. 2022). However, this result changed when comparing equivalent areas of corrugated panels 1910eq. The corrugation process deteriorated the veneers, making them 25% more permeable than plywood (Copak *et al*. 2022).
5. Corrugated panels exhibited typical wood-based behavior for sorption/desorption in their inner material. They tend to absorb less moisture than plywood, with 1910_f panels absorbing up to 33% less moisture for 50% RH and 48% less moisture for 90% RH in sorption (Kumaran 2006).
6. Corrugated panels exhibited high moisture buffer values due to their higher surface area. For example, 1910_{ap} panels had a moisture buffer value about 261% higher than plywood with a thickness of 12.7 mm (Wu *et al*. 2008), concerning their inner thickness of about 2 mm.
7. The 1910 panel was the most promising for applications in the built environment, as it exhibited the least sensitivity to liquid water or water vapor.

The results of this study show that the panels tested had properties similar to plywood panels, which are widely used in the construction industry. Thus, with their original shape, corrugated panels could open up new possibilities and applications in building envelopes.

ACKNOWLEDGMENTS

The authors are thankful to the Natural Sciences and Engineering Research Council (NSERC) of Canada for the financial support through its IRC and CRD programs (IRCPJ 461745-18 and RDCPJ 524504-18) as well as the industrial partner, Corruven Inc., of the NSERC industrial chair on eco-responsible wood construction (CIRCERB). A sincere gratitude to the master's intern Clémence Grand from Polytech Annecy-Chambéry for assisting in the laboratory work and all laboratory technicians of the renewable materials research center (CRMR).

REFERENCES CITED

Acharya, M., Naderi, M., Burnett, D., and Dienstmaier, J. (2014). *DVS Application note 61 - Characterizing the Restoration Materials for Historic Buildings Using Dynamic Vapour Sorption Technique*.

Adl-Zarrabi, B., and Boström, L. (2004). Determination of Thermal Properties of Wood and Wood Based Products by Using Transient Plane Source. in: *Proceedings of the 8th World Conference on Timber Engineering*, p. 604.

Ajeel, R. K., and Salim, W. S. I. W. (2021). "Experimental assessment of heat transfer and pressure drop of nanofluid as a coolant in corrugated channels," *J. Therm. Anal. Calorim.* 144(4), 1161-1173. DOI: 10.1007/s10973-020-09656-1

Almeida, G., Rémond, R., and Perré, P. (2018). "Hygroscopic behaviour of lignocellulosic materials: Dataset at oscillating relative humidity variations," *Journal of Building Engineering* 19, 320-333. DOI: 10.1016/j.jobe.2018.05.005

Al Zahrani, S., Islam, M. S., Xu, F., and Saha, S. C. (2020). "Thermal performance investigation in a novel corrugated plate heat exchanger," *Int. J. Heat Mass Transf.* 148, article 119095. DOI: 10.1016/j.ijheatmasstransfer.2019.119095

ASTM C1058/1058M-10 (2015). "Standard practice for selecting temperatures for evaluating and reporting thermal properties of thermal insulation," ASTM International, West Conshohocken, PA, USA.

ASTM E96/E96M-16 (2016). "Standard test methods for water vapor transmission of materials," ASTM International, West Conshohocken, PA, USA.

ASTM C1498 − 04a (2016). "Standard test method for hygroscopic sorption isotherms of building materials," ASTM International, West Conshohocken, PA, USA.

ASTM C518-17 (2017). "Standard test method for steady-state thermal transmission properties by means of the heat flow meter apparatus," ASTM International, West Conshohocken, PA, USA.

ASTM E1269 - 11 (2018). "Standard test method for determining specific heat capacity by differential scanning calorimetry," ASTM International, West Conshohocken, PA, USA.

ASTM C177-19 (2019). "Standard test method for steady-state heat flux measurements and thermal transmission properties by means of the guarded-hot-plate," ASTM International, West Conshohocken, PA, USA.

ASTM C1794-19 (2019). "Standard test methods for determination of the water absorption coefficient by partial immersion," ASTM International, West Conshohocken, PA, USA.

Bapanapalli, S. K., Martinez, O. M., Gogu, C., Sankar, B. V, Haftka, R. T., and Blosser, M. L. (2006). (Student paper) "Analysis and design of corrugated-core sandwich panels for thermal protection systems of space vehicles," in: *47th AIAA/ASME/ASCE/AHS/ASC Structures, Structural Dynamics, and Materials Conference 14th AIAA/ASME/AHS Adaptive Structures Conference*, 7th (p. 1942).

Belanger, A., and Blais, M. (2010). *Wave Wood Assembly and Method of Making Same*, Corruven Canada Inc., Canada.

Burnett, D., Garcia, A. R., Naderi, M., and Acharya, M. (1996). *DVS Application Note 104 Vapour Sorption Properties of Building Materials using Gravimetric Sorption Instrumentation-an Overview*.

Carmeliet, J., De Wit, M., and Janssen, H. (2005, June). "Hysteresis and moisture buffering of wood," in: Symposium of Building Physics in the Nordic Countries, pp. 55-62.

Chen, Y., Zhang, L., He, C., He, R., Xu, B., and Li, Y. (2021). "Thermal insulation performance and heat transfer mechanism of C/SiC corrugated lattice core sandwich panel," *Aerosp Sci Technol*. 111, article 106539. DOI: 10.1016/j.ast.2021.106539

Choi, S. W., Park, S. H., Jeong, H. S., Cho, J. R., Park, S., and Ha, M. Y. (2012). "Improvement of formability for fabricating thin continuously corrugated structures in sheet metal forming process," *Journal of Mechanical Science and Technology* 26(8), 2397-2403. DOI: 10.1007/s12206-012-0616-z.

Copak, A., Jirouš-Rajković, V., Živković, V., and Miklečić, J. (2022). "Water vapour transmission properties of uncoated and coated wood-based panels," *Wood Mater Sci Eng*, 1-8. DOI: 10.1080/17480272.2022.2106582

Cunha, S., Pinto, J., Paiva, A., Briga-Sá, A., Soares, N., Varum, H., and Ferreira, D. (2015). "A contribution for the improvement in thermal insulation of tabique walls coated with metal corrugated sheets," *Building Services Engineering Research and Technology* 36(4), 439-454. DOI: 10.1177/0143624414558720

Czajkowski, Ł., Olek, W., Weres, J., and Guzenda, R. (2016). "Thermal properties of wood-based panels: specific heat determination," *Wood Sci Technol*. 50(3), 537-545. DOI: 10.1007/s00226-016-0803-7

Denes, L., Lang, E. M., and Mcneel, J. F. (2017a). "Development of veneer-based corrugated composites, Part 1: Manufacture and basic material properties," *BioResources* 12(1), 774-784. DOI: 10.15376/biores.12.1.774-784

Denes, L., Lang, E. M., Mcneel, J. F., and Mcgraw, B. (2017b). "Development of veneer-based corrugated composites, Part 2: Evaluation of structural joints and applications," *BioResources* 12(2), 3478-3489. DOI: 10.15376/biores.12.2.3478-3489

Doo, J. H., Ha, M. Y., Min, J. K., Stieger, R., Rolt, A., and Son, C. (2012). "Theoretical prediction of longitudinal heat conduction effect in cross-corrugated heat exchanger," *Int. J. Heat Mass Transf.* 55(15-16), 4129-4138. DOI: 10.1016/j.ijheatmasstransfer.2012.03.054

Dupleix, A., Kusiak, A., Hughes, M., and Rossi, F. (2013). "Measuring the thermal properties of green wood by the transient plane source (TPS) technique," *Holzforschung* 67(4), 437-445. DOI: 10.1515/hf-2012-0125

Garbowski, T., Knitter-Piątkowska, A., and Grabski, J. K. (2023). "Estimation of the edge crush resistance of corrugated board using artificial intelligence," *Materials* 16(4), article 1631. DOI: 10.3390/ma16041631.

Ge, H., Yang, X., Fazio, P., and Rao, J. (2014). "Influence of moisture load profiles on moisture buffering potential and moisture residuals of three groups of hygroscopic materials," *Build Environ*. 81, 162-171. DOI: 10.1016/j.buildenv.2014.06.021

Gray-Stuart, E. M., Bronlund, J. E., Navaranjan, N., and Redding, G. P. (2019). "Measurement of thermal conductivity of paper and corrugated fibreboard with prediction of thermal performance for design applications," *Cellulose* 26(9), 5695-5705. DOI: 10.1007/s10570-019-02462-5

Innocenti, P., and Scarpa, F. (2009). "Thermal conductivity properties and heat transfer analysis of multi-re-entrant auxetic honeycomb structures," *J. Compos. Mater*. 43(21), 2419-2439. DOI: 10.1177/0021998309344636

ISO 24353 (2008). "Hygrothermal performance of building materials and products — Determination of moisture adsorption/desorption properties in response to humidity variation," International Organization for Standardization, Geneva, Switzerland.

Iwai, H., Tatsumi, K., and Suzuki, K. (2006). "Effect of the plate thermal resistance on the heat transfer performance of a corrugated thin plate heat exchanger," *Heat Transfer - Asian Research* 35(3), 209-223. DOI: 10.1002/htj.20110

Jiloul, A., Blanchet, P., and Boudaud, C. (2023). "Mechanical characterization of corrugated wood-based panels and potential structural applications in a building," *Constr. Build. Mater.* 391, article 131896. DOI: 10.1016/j.conbuildmat.2023.131896

Kawasaki, T., Zhang, M., and Kawai, S. (1998). "Manufacture and properties of ultra-low-density fiberboard," *Journal of Wood Science* 44, 354-360.

Kittisak, B., and Prayoon, S. (2021). "Properties of corrugated roofing sheet material from sugarcane bagasse fibers," *J. Phys. Conf. Ser*. 1860(1), article 012007). IOP Publishing Ltd.

Klinklow, N., Padungkul, S., Kanthong, S., Patcharaphun, S., and Techapiesancharoenkij, R. (2013). "Development of a kraft paper box lined with thermal-insulating materials by utilizing natural wastes," *Key Eng Mater*, 545, 82-88.

Kumaran, M. K. (2006). *A Thermal and Moisture Property Database for Common Building and Insulation Materials*. ASHRAE transactions, 112(2).

Kumaran, M. K., Lackey, J. C., Normandin, N., Tariku, F., and Van Reenen, D. (2010). "Variations in the hygrothermal properties of several wood-based building products," *Research in Building Physics*, 10.

Le, V. T., and Goo, N. S. (2019). "Thermomechanical performance of bio-inspired corrugated-core sandwich structure for a thermal protection system panel," *Applied Sciences (Switzerland)* 9(24), article 5541. DOI: 10.3390/app9245541

Liu, K., Zong, S., Li, Y., Wang, Z., Hu, Z., and Wang, Z. (2022). "Structural response of the U-type corrugated core sandwich panel used in ship structures under the lateral quasi-static compression load," *Marine Structures* 84, article 103198. DOI: 10.1016/j.marstruc.2022.103198

Lu, J., Wang, K., and Qu, M. L. (2020). "Experimental determination on the capillary water absorption coefficient of porous building materials: A comparison between the intermittent and continuous absorption tests," *Journal of Building Engineering* 28, article 101091. DOI: 10.1016/j.jobe.2019.101091

Lurie, S., Volkov-Bogorodskiy, D., Solyaev, Y., Koshurina, A., and Krasheninnikov, M. (2020). "Impact behavior of a stiffened shell structure with optimized GFRP corrugated sandwich panel skins," *Compos Struct* 248. DOI: 10.1016/j.compstruct.2020.112479

Ma, Y., Xu, B., Chen, M., He, R., Wen, W., Cheng, T., and Fang, D. (2017). "Optimization design of built-up thermal protection system based on validation of corrugated core homogenization," *Appl Therm Eng* 115, 491-500. DOI: 10.1016/j.applthermaleng.2016.12.137

McCracken, A., and Sadeghian, P. (2018). "Corrugated cardboard core sandwich beams with bio-based flax fiber composite skins," *Journal of Building Engineering* 20, 114-122. DOI: 10.1016/j.jobe.2018.07.009

Mohammadabadi, M., Jarvis, J., Yadama, V., and Cofer, W. (2020). "Predictive models for elastic bending behavior of a wood composite sandwich panel," *Forests* 11(6), 624. DOI: 10.3390/F11060624

Mrówczyński, D., Gajewski, T., and Garbowski, T. (2023). "Sensitivity analysis of open-top cartons in terms of compressive strength capacity," *Materials* 16(1). DOI: 10.3390/ma16010412.

Mvondo, R. R. N., Damfeu, J. C., Meukam, P., and Jannot, Y. (2020). "Influence of moisture content on the thermophysical properties of tropical wood species," *Heat and Mass Transfer/Waerme- und Stoffuebertragung* 56(4), 1365-1378. DOI: 10.1007/s00231-019-02795-8

Nopens, M., Sazama, U., Krause, A., and Fröba, M. (2021). "Specific heat capacity of wood between -140 and 50 °C in dry and wet state," *Holzforschung* 75(9), 779-785. DOI: 10.1515/hf-2020-0204

Osanyintola, O. F., Talukdar, P., and Simonson, C. J. (2006). "Effect of initial conditions, boundary conditions and thickness on the moisture buffering capacity of spruce plywood," *Energy Build*. 38(10), 1283-1292. DOI: 10.1016/j.enbuild.2006.03.024

Pinterić, M. (2017). *Building Physics : From physical principles to international standards*. Maribor: Springer. 112-114.

Radmanović, K., Dukić, I., and Pervan, S. (2014). "Specific heat capacity of wood," *Drvna Industrija* 65(2). DOI:10.5552/drind.2014.1333

Rice, R. W., and Redfern, I. (2016). "Heat capacity and its variation with moisture content for plywood and oriented strand board sheathing produced by North American mills," *For Prod J*. *66*(7-8), 413-418. DOI: 10.13073/FPJ-D-15-00062

Rode, C., Mortensen, R. H., Hansen, L. H., Ojanen, A., Svennberg, J., and Harderup, J. (2005). *Moisture Buffering of Building Materials* (BYG Report No. R-127), Technical University of Denmark, Kongens Lyngby, Denmark.

Sasaki, H., and Kato, E. (1999). "Heat insulating cardboard composed of corrugated foamed polystyrene layer," *Packaging Technology and Science* 12(3), 151-157. DOI: 10.1002/(SICI)1099-1522(199905/06)12:3<151::AID-PTS463>3.0.CO;2-R

Sattler, S., and Österreicher, D. (2019). "Assessment of sustainable construction measures in building refurbishment-life cycle comparison of conventional and Multi-Active Façade systems in a social housing complex," *Sustainability (Switzerland)* 11(16), article 4487. DOI: 10.3390/su11164487

Shi, S., Wang, Y., Yan, L., Sun, P., Li, M., and Tang, S. (2020). "Coupled ablation and thermal behavior of an all-composite structurally integrated thermal protection system: Fabrication and modeling," *Compos Struct*. 251, article 112623. DOI: 10.1016/j.compstruct.2020.112623

Skaar, C. (1988). *Wood-Water Relations*, Springer Science & Business Media, Berlin Heidelberg.

Sonderegger, W., Häring, D., Joščák, M., Krackler, V., and Niemz, P. (2012). "Untersuchungen zur Wasseraufnahme von Vollholz und Holzwerkstoffen," *Bauphysik* 34(3), 101-106. DOI: 10.1002/bapi.201200014

Sonderegger, W., Hering, S., and Niemz, P. (2011). "Thermal behaviour of Norway spruce and European beech in and between the principal anatomical directions," *Holzforschung* 65(3), 369-375. DOI: 10.1515/HF.2011.036

Sonderegger, W., and Niemz, P. (2009). "Thermal conductivity and water vapour transmission properties of wood-based materials," *European Journal of Wood and Wood Products* 67(3), 313-321. DOI: 10.3929/ethz-b-000021316

Tleoubaev, A., and Brzezinski, A. (2008). "Errors of the heat flow meter method caused by thermal contact resistance for thermal conductivity," in: *Joint 29th International Thermal Conductivity Conference/17th International Thermal Expansion Symposium*, Birmingham, AL, USA, pp. 465-473.

VaproShield LLC (2022). "Product Data Sheet : WallShield IT ® Integrated Tape," Gig Harbor.

Vololonirina, O., and Perrin, B. (2016). "Inquiries into the measurement of vapour permeability of permeable materials," *Constr. Build. Mater*. 102, 338-348. DOI: 10.1016/j.conbuildmat.2015.10.126

von der Heyden, A., and Lange, J. (2017). "07.25: Assessment of the utilisation of corrugated cardboard as a core material for sandwich panels," *ce/papers* 1 (2–3), 1716-1725. DOI: 10.1002/cepa.215

Voth, C., White, N., Yadama, V., and Cofer, W. (2015). "Design and evaluation of thin-walled hollow-core wood-strand sandwich panels," *J. Renew. Mater*. 3(3), 234-243. DOI: 10.7569/JRM.2015.634109

Wu, Y., Fazio, P., and Kumaran, M. (2008). "Moisture buffering capacities of five North American building materials," *Journal of Testing and Evaluation* 36(1), 34-40. DOI: 10.1520/JTE101228

Zahedsheijani, R., Faezipour, M., Tarmian, A., Layeghi, M., and Yousefi, H. (2012). "The effect of Na^+ montmorillonite (NaMMT) nanoclay on thermal properties of medium density fiberboard (MDF)," *European Journal of Wood and Wood Products* 70 (5), 565-571. DOI: 10.1007/s00107-011-0583-6

Zelinka, S. L., Glass, S. V., and Boardman, C. R. (2016). "Improvements to water vapor transmission and capillary absorption measurements in porous materials," *J. Test Eval*. 44(6), 2396-2402. DOI: 10.1520/JTE20150209

Zhang, M., Qin, M., Rode, C., and Chen, Z. (2017). "Moisture buffering phenomenon and its impact on building energy consumption," *Appl. Therm. Eng*. 124, 337-345. DOI: 10.1016/j.applthermaleng.2017.05.173

Zhang, W., Wang, J., Mahdavian, M., and Yu, C. (2016). "Seismic performance of cold-formed steel framed buildings using corrugated sheet shear walls," in: *Geotechnical and Structural Engineering Congress 2016*, Phoenix, AZ, USA. 252-263. DOI: 10.1061/9780784479742.021

Zhou, X. Y., Zheng, F., Li, H. G., and Lu, C. L. (2010). "An environment-friendly thermal insulation material from cotton stalk fibers," *Energy Build*. 42(7), 1070-1074. DOI: 10.1016/j.enbuild.2010.01.020

Article submitted: June 12, 2023; Peer review completed: July 1, 2023; Revised version received and accepted: July 7, 2023; Published: July 14, 2023.
DOI: 10.15376/biores.18.3.5838-5858